Results in Physics 12 (2019) 662–672

Contents lists available at ScienceDirect

Results in Physics

journal homepage: www.elsevier.com/locate/rinp

Research on the novel explicit model for photovoltaic I-V characteristic of the single diode model under different splitting spectrum

Luqing Liu[a,b,*], Wen Liu[a,b], Xinyu Zhang[a], Jan Ingenhoff[b]

[a] Optics and Optical Engineering Department, University of Science and Technology of China, Hefei, China
[b] Institute of Advanced Technology, Hefei, China

ARTICLE INFO

Keywords:
Photovoltaic panel
Explicit model
Spectrum splitting
I-V characteristic prediction
Shape parameter

ABSTRACT

Photovoltaic (PV) panel has been widely used in many spectrum splitting systems. However the spectrum splitting normally discussed only with photocurrent. In this paper, the relationship between the current-voltage (I-V) curve and the irradiation spectrum is discussed by combining the single diode model. An explicit elementary analytical model with two defined shape parameters is improved with three approximations and second order Taylor expansion. The relationship between the physical parameters and the condition parameters is applied to extract the shape parameters at different scenarios. Considering the aging effect, the process of calculation to predict I-V curve is simplified as follow: (1) two shape parameters are gotten from I-V data at measurement reference conditions (MRC); (2) short circuit current, open circuit voltage and shape parameters under any splitting spectrum can be calculated based on the relationship provided in article; (3) the performance of PV panel can be predicted with parameters. The validation of this model was experimentally proven leveraging monocrystalline silicon photovoltaic module with different splitting films. Moreover, the presented model performs superior compared to other investigated models when looking at accuracy and simplicity.

Introduction

Photovoltaic power generation technology was greatly improved and widely used all over the world since it has been invented [1]. As the photovoltaic cell can't utilize all the wavelengths of sunlight effectively, there are many systems combining several kinds of photovoltaic cells emerged to get a higher system efficiency. The idea of utilizing specific ranges of sunlight spectrum for various kinds of photovoltaic cells was firstly presented in 1955 by Jackson [2] and firstly experimentally demonstrated in 1978 by Moon et al. [3]. Many studies were carried out in this field to improve the efficiency of photovoltaic systems [4–7]. Additionally, many papers about Hybrid Photovoltaic (PV)-Thermoelectric (TE) systems which is another kind of splitting technology also emerged in recent years. The PV-TE systems make part of solar radiation available for PV generating system [8]. The rest of solar radiation is concentrated on the TE system for producing electricity through the thermoelectric effect. Thus the PV-TE systems further reduce the heat at the solar cells and improve the efficiency of the whole systems [9,10]. On the other hand, photovoltaic power generating systems can be also combined with some concepts other than power generating. For example, a photovoltaic-greenhouse system had been proposed by Sonneveld et al. [11,12]. In this case, photosynthetically active radiation is transmitted through the film that is coated on the glass roof of green houses for plant growth. The film has a total reflection in the near infrared (NIR) region. Therefore, solar panels can leverage NIR that is reflected and concentrated for power generation. For the systems with different combinations, the spectra of beam splitting are quite diverse. This situation requests an effective and precise way to predict I-V curve of the PV panel under different irradiation spectra.

To get I-V curve for a PV panel, a circuital equivalent model is needed. Among the models which are used in the papers for PV panel simulation, the one diode equivalent representation model is more common than other models such as two/three diodes equivalent representation models. This single diode model is also well known as five-parameter model since I-V curve in this model is determined by five parameters [13–15]. The equation received directly from the single diode model is a transcendental equation that is implicit. Therefore, the exact analytic solution of I-V curve can't be obtained directly. Many approaches have been carried out to extract the parameters in the single diode model [16,17]. Because of the complexity of the implicit model, the calculation of the I-V curve normally requires the parameters from the manufacture data sheet and it takes more time to approach the

Abbreviations: MRC, measurement reference conditions; SRC, standard reference conditions; PV, Photovoltaic; TE, Thermoelectric

* Corresponding author.
E-mail address: llq77@mail.ustc.edu.cn (L. Liu).

https://doi.org/10.1016/j.rinp.2018.12.021
Received 7 November 2018; Received in revised form 2 December 2018; Accepted 2 December 2018
Available online 07 December 2018

Nomenclature

I_{ph}	photocurrent
R_{sh}	shunt resistance
R_s	series resistance
I_0	saturation current
n	ideality factor of diode
V_{cell}	voltage of solar cell
$R_{s,cell}$	series resistance of solar cell
$R_{sh,cell}$	shunt resistance of solar cell
V_T	thermal voltage
T	absolute temperature
k	Boltzmann constant
q	electronic charge
N_s	Number of solar cells in series
v	normalized voltage
i	normalized current
V_{oc}	open circuit voltage
I_{sc}	short circuit current
γ	linear parameter
m	exponent parameter
i_{mp}	normalized current at maximum point
v_{mp}	normalized voltage at maximum point
θ	calibration parameters
K_{ph}	photocurrent ratio parameter
K_0	saturation current ratio parameter
K_{sh}	shunt resistance ratio parameter
K_s	series resistance ratio parameter
k_1	spectral ratio parameter
$Spl(\lambda)$	splitting spectrum separation function
$Rs(\lambda)$	spectrum response function
$Spe(\lambda)$	solar irradiation spectrum function
V_{oc}^{MRC}	open circuit voltage at MRC
I_{sc}^{MRC}	short circuit current at MRC
γ^{MRC}	linear parameter at MRC
m^{MRC}	exponent parameter at MRC
α_{ph}	slope parameter of short-current and temperature
β_{oc}	slope parameter of voltage and temperature
E_g	band gap
S	solar irradiation intensity
S^{MRC}	solar irradiation intensity at MRC

output current with the voltage of PV cells or panels. Many methods of the analytical explicit model of I-V characteristic have been investigated in the last two decades [18–25]. One kind of these methods expressing I-V characteristic based on the Lambert W-function. This method is an exact expression derived from the physical model [15,26]. The other methods are in terms of elementary approach. The models based on these methods are more widely used in the practical application because of their simplified form. Karmalkar et al. presented an explicit model with defined shape parameters. They combined the explicit models and the single diode model to identify the relationship between the five physical parameters and defined the shape parameters [18,21]. With this relationship, the five physical parameters can be calculated or numerically approximated with just few measurements. Furthermore, the whole I-V curve and maximum operating point of the PV panel can be determined without tracking the output current and voltage until open circuit from short circuit.

PV systems are used under multiple conditions. It is well known that the efficiency of PV cells decreases with increasing temperature as well as decreasing light intensity. There are many studies discussing the mathematical model of this phenomenon. In PV systems with spectral separation, the spectral response of the solar cells is typically used only to determine the photocurrent [5]. The changing irradiation spectrum is converted into the changing light intensity so that the photocurrent can be obtained under different spectrum conditions [5,27,28]. Based on the relationship between the five parameters and operating conditions, a model can be developed to predict I-V curve. Yunpeng Zhang et al. put forward a flexible and reliable method leveraging several measurements at MRC. This method is convenient for the practical application with the changing physical parameters in the photovoltaic panel working life [29].

In this paper, a simplified elementary method for a PV panel is proposed which can predict I-V characteristic under varying spectral conditions with two defined shape parameters. This explicit expression is directly derived from a physical model and acts more effectively onerror reduction compared to previous methods. The two defined shape parameters are expressed directly through the measurements at MRC and the splitted spectrum. The relationship between shunt resistance and irradiation spectrum is discussed combining the spectral response. Considering the aging effect, the process of calculation to predict the I-V curve under different splitting spectra is simplified as follow: (1) two shape parameters are gotten from the I-V data at MRC; (2) the short circuit current, open circuit voltage and shape parameters under any splitting spectrum can be calculated based on the relationship provided in article; (3) the performance of PV panel can be predicted with parameters. At the end of paper, the model are validated through the experiments with seven kinds of films. The reliability of the model is proved by the result of the validation experiments.

The single diode model is discussed and simplified in part 2 and 3. Then the method is discussed in part 4 with varying conditions, especially with different spectrum splitting. The method is validated and the result of experiment is discussed in part 5.

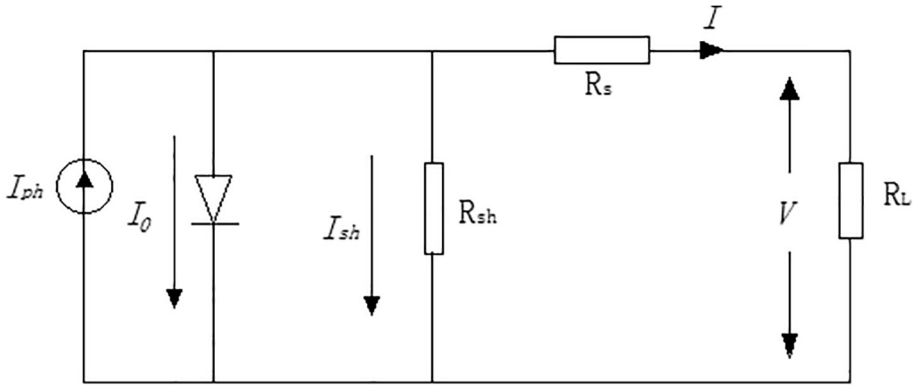

Fig. 1. The equivalent single diode model for a PV panel or a solar cell.

Materials and methods

Single diode model

The physical model of a solar cell in a solar panel can be described as a single diode model such as shown in Fig. 1. The model contains a light-induced current source, an ideal diode, a series resistance and a shunt resistance. The light-induced current source provides photocurrent when the irradiation reaches the surface of solar cells based on photoelectric conversion. As it is well known, this model has five parameters: photocurrent (I_{ph}), shunt resistance (R_{sh}), series resistance (R_s), saturation current under reverse bias (I_0) and the ideality factor of diode (n).

With those five parameters, the equation of I-V curve for a solar cell is:

$$I = I_{ph} - I_0\left(e^{\frac{V_{cell}+IR_{s,cell}}{nV_T}} - 1\right) - \frac{V_{cell} + IR_{s,cell}}{R_{sh,cell}} \tag{1}$$

In the Eq. (1), V_T is equal to kT/q, in which k is Boltzmann constant (1.381×10^{-23} J/K) and q is the electronic charge (1.608×10^{-19} C). T is the absolute temperature in Kelvin which is 298.15 K at SRC conditions. The parameters in the equation for a solar panel with N_s identical solar cells in series can be modified as follow equations.

$$V = N_s V_{cell} \tag{2}$$

$$R_s = N_s R_{s,cell} \tag{3}$$

$$R_{sh} = N_s R_{sh,cell} \tag{4}$$

The Eqs. (2) and (3) are suitable for varying kinds of solar cells, including monocrystalline silicon and polycrystalline silicon. In the series circuit, the total current is equal to the current of each component. Then equation of the I-V curve for a solar panel with N_s identical solar cells in series should be changed into the form as Eq. (5).

$$I = I_{ph} - I_0\left(e^{\frac{V+IR_s}{N_s nV_T}} - 1\right) - \frac{V + IR_s}{R_{sh}} \tag{5}$$

Explicit elementary analytical model with two defined shape parameters

Defining the normalized voltage v and normalized current i via the short circuit current I_{sc} and open circuit voltage V_{oc} derives in the following equations

$$v = V/V_{oc} \tag{6}$$

$$i = I/I_{sc} \tag{7}$$

Putting Eqs. (5) and (6) into Eq. (7), the Eq. (7) can be expressed as follow:

$$i = 1 - \frac{I_0}{I_{sc}}\left[\exp\left(\frac{V + IR_s}{N_s nV_T}\right) - \exp\left(\frac{I_{sc}R_s}{N_s nV_T}\right)\right] - \frac{(I - I_{sc})R_s + V}{R_{sh}I_{sc}} \tag{8}$$

To simplify the Eq. (8), three approximations are possible:

I. Approximation 1 is about the term $\frac{(I-I_{sc})R_s}{R_{sh}I_{sc}}$.

Because the series resistance R_s is much smaller than the shunt resistance in solar cells (normally $R_s/R_{sh} < 10^{-3}$), the term is far less than 1 and approximately equal to 0.

$$\frac{(I_{sc} - I)R_s}{I_{sc}R_{sh}} \leqslant \frac{R_s}{R_{sh}} << 1 \tag{9}$$

Thus, this term can be ignored.

II. Approximation 2 is about the term $\frac{I_0}{I_{sc}}\exp\left(\frac{I_{sc}R_s}{N_s nV_T}\right)$

Considering short circuit condition with $V = 0$ and place it into Eq. (5), this part can be expressed as Eq. (10).

$$\frac{I_0}{I_{sc}}\exp\left(\frac{I_{sc}R_s}{N_s nV_T}\right) = \frac{I_0}{I_{sc}} - \frac{R_s}{R_{sh}} + \left(\frac{I_{ph}}{I_{sc}} - 1\right) < \frac{I_0}{I_{sc}} + \frac{I_{ph}}{I_{sc}} - 1 \tag{10}$$

For most solar cells, the value of saturation current is much lower than output current so that $I_0/I_{sc} << 1$ (normally $I_0/I_{sc} < 10^{-4}$). Furthermore, normally the value of I_{ph} is approximately equal to the value of the output current I_{sc}. Therefore, we can get $I_{ph}/I_{sc} \approx 1$. Thus, this term can be approximately ignored because of $\frac{I_0}{I_{sc}}\exp\left(\frac{I_{sc}R_s}{N_s nV_T}\right) << 1$.

III. Approximation 3 is about the term $\frac{I_0}{I_{sc}}\exp\left(\frac{V+IR_s}{N_s nV_T}\right)$

Considering both short circuit condition and open circuit. Place $I = 0$ when $V = V_{oc}$ and $V = 0$ when $\mathbf{I = I_{sc}}$ condition into Eq. (5), the form of the term $\frac{I_0}{I_{sc}}\exp\left(\frac{V+IR_s}{N_s nV_T}\right)$ can be transformed in the following way

$$\frac{I_0}{I_{sc}}\exp\left(\frac{V + IR_s}{N_s nV_T}\right) \approx \left(1 - \frac{V_{oc}}{I_{sc}R_{sh}}\right)[\exp(v-1)]^{\frac{V_{oc}}{N_s nV_T}\cdot\left(1-\frac{IR_s}{V_{oc}-V}\right)} \tag{11}$$

After transforming into Eq. (11), the $\left(1 - \frac{IR_s}{V_{oc}-V}\right)$ is considered a voltage independent constant. The error caused by approximation 3 is the main error in this model. However, the error can be reduced by adjusting the expression of the term $\frac{V_{oc}}{N_s nV_T}\cdot\left(1 - \frac{IR_s}{V_{oc}-V}\right)$

After these three approximations as shown above, the Eq. (8) can be changed into (12)

$$i = 1 - \frac{V_{oc}}{R_{sh}I_{sc}}v - \left(1 - \frac{V_{oc}}{I_{sc}R_{sh}}\right)[\exp(v-1)]^{\frac{V_{oc}}{N_s nV_T}\cdot\left(1-\frac{IR_s}{V_{oc}-V}\right)} \tag{12}$$

Then it is easy to see that the Eq. (12) can be simplified with two defined parameters (linear parameterγand exponent parameter m) as follows:

$$i = 1 - (1-\gamma)v - \gamma[\exp(v-1)]^m \tag{13}$$

The form of Eq. (13) can be simplified by a Taylor exponent expending row:

$$i = 1 - (1-\gamma)v - \gamma\left[1 + (v-1) + \frac{1}{2!}(v-1)^2 + \frac{1}{3!}(v-1)^3 \ldots + \frac{1}{N!}(v-1)^N \ldots\right]^m \tag{14}$$

If the Eq. (14) is approximated in the first order, it can be modified into Eq. (15).

$$i = 1 - (1-\gamma)v - \gamma v^m \tag{15}$$

This form of the explicit I-V model is provided and discussed by Karmalkar et al. and allows an easy closed-form estimation of the entire I-V curve [18,30]. The predictability of this method was verified, and the scope was expanded to a wide range of solar cells made out of various materials [31]. The two defined shape parameters can be derived from few measurement I-V points as well as five physical parameters in the single diode model. There is an explicit elementary expression with two shape parameters in this analyze method for the fill factor and the maximum power point. This method is proved that it fits better than the other methods for describing the performance of a PV panel [32]. The method can be widely used in practical applications because of the easy calculation avoiding the difficulty of measurements and numerical approaching in parameter extraction. This method can be improved by adding the second-order term in the Taylor expansion. In this way, the Eq. (13) can be changed into Eq. (16)

$$i = 1 - (1-\gamma)v - \gamma\left(\frac{v^2+1}{2}\right)^m \tag{16}$$

In this explicit analysis of I-V form, the normalized current i_{mp} and normalized voltage v_{mp} at maximum point can be gotten by:

$$\left.\frac{d(iv)}{di}\right|_{i=i_{mp}} = 0 \tag{17}$$

Table 1
Shape parameters of measurement data at MRC of S = 880 W/m^2, T = 285 K.

Shape Parameters	Value
Short-circuit current I_{sc} (A)	5.368
Open-circuit voltage V_{oc} (V)	5.280
Exponent parameter m	24.58
Linear parameter γ	0.982

$$\left.\frac{d(iv)}{dv}\right|_{v=v_{mp}} = 0 \tag{18}$$

Then i_{mp} and v_{mp} are represented as follow:

$$v_{mp} = (m+1)^{-\frac{1}{m}} - 0.05(1-\gamma) \tag{19}$$

$$i_{mp} = 1 - (1-\gamma)v_{mp} - \gamma\left(\frac{v_{mp}^2+1}{2}\right)^m \tag{20}$$

The Eqs. (16), (19) and (20) can express the I-V characteristic and maximum point with I_{sc} and V_{oc} while the I_{sc} and V_{oc} can be measured directly. Some manufacturers provide the five physical parameters of the solar cell at SRC. Of course, the two shape parameters m and γ can be extracted by the five physical parameters containing all the information of the I-V curve. The linear parameter γ is defined by the Eqs. (12) and (13) as:

$$\gamma = 1 - \frac{V_{oc}}{I_{sc}R_{sh}} \tag{21}$$

The exponent parameter m is defined in approximation 3 (see above) and the value can be determined by the derivative at the open-circuit point of the I-V curve to reduce the error as this has been mentioned in Karmalkar S, (2008).

$$\left.\frac{I_{sc}}{V_{oc}}\frac{di}{dv}\right|_{i=0} = \left.\frac{dI}{dV}\right|_{I=0} \tag{22}$$

Putting the Eqs. (5) and (16) into the Eq. (22), the expression of m is as follows

$$m = 1 - \frac{1}{\gamma} + \frac{V_{oc}}{N_s n V_T + \gamma I_{sc}R_s} \tag{23}$$

Furthermore, the value of m is adjusted by a calibration parameter θ in the explicit model of Karmalkar (2008, 2009) [18,29] in order to reduce the error which can't be avoided between the implicit model and the explicit model. The expression for the parameter m with θ was changed into the Eq. (24).

$$m = 1 - \frac{1}{\gamma} + \frac{V_{oc}}{N_s n V_T + \theta\gamma I_{sc}R_s} \tag{24}$$

θ is an empirical value without any physical meaning and the value can be approximately represented by $\theta \approx 0.77 i_{mp}\gamma$. The expression contains current ratio at the maximum power point i_{mp} so it can't be used for the prediction. Considering both short circuit condition and open circuit in the Eq. (5), I_{sc} and V_{oc} are expressed by the five physical parameters in the forms as follow:

$$I_{sc} \approx I_{ph}\left(1 + \frac{R_s}{R_{sh}}\right)^{-1} \tag{25}$$

$$V_{oc} \approx N_s n V_T \ln\left[\frac{I_{ph}}{I_0} - \frac{N_s n V_T}{R_{sh}I_0}\ln\left(\frac{I_{ph}}{I_0}\right)\right] \tag{26}$$

Explicit elementary analytical under varying conditions

In the single diode model, four parameters I_{ph}, I_0, R_s and R_{sh} are considered to be related to temperature and irradiation intensity. By defining the ratio of these four parameters at different conditions with varying temperature and irradiation, the following equations result:

$$K_{ph} = \frac{I_{ph}}{I_{ph}^{MRC}} \tag{27}$$

$$K_0 = \frac{I_0}{I_0^{MRC}} \tag{28}$$

$$K_{sh} = \frac{R_{sh}}{R_{sh}^{MRC}} \tag{29}$$

$$K_s = \frac{R_s}{R_s^{MRC}} \tag{30}$$

the expression of short-circuit current $I_{sc,}$ open-circuit voltage V_{oc} and two shape parameters m and γ can be changed into Eqs. (31)–(34) deriving from Eqs. (21), (23), (25), (26) with the value of parameters at MRC and Eqs. (27)–(30).

$$I_{sc} \approx K_{ph} I_{sc}^{MRC} \tag{31}$$

$$V_{oc} \approx \frac{T}{T^{MRC}}V_{oc}^{MRC} + N_s n V_T(\ln K_{ph} - \ln K_0) \tag{32}$$

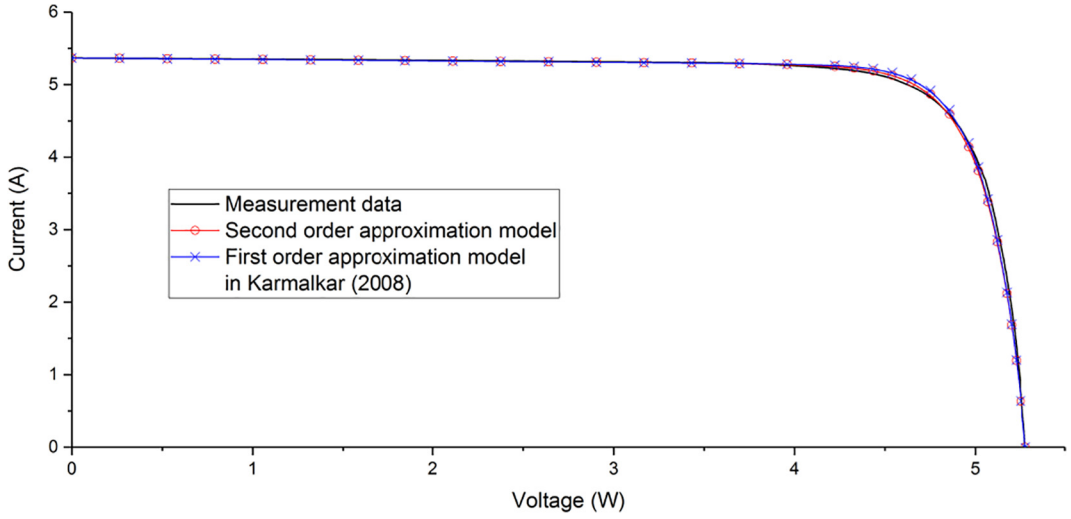

Fig. 2. The I-V curve with measurement data, simulated data of improved model and simulated data of model in Karmalkar (2008).

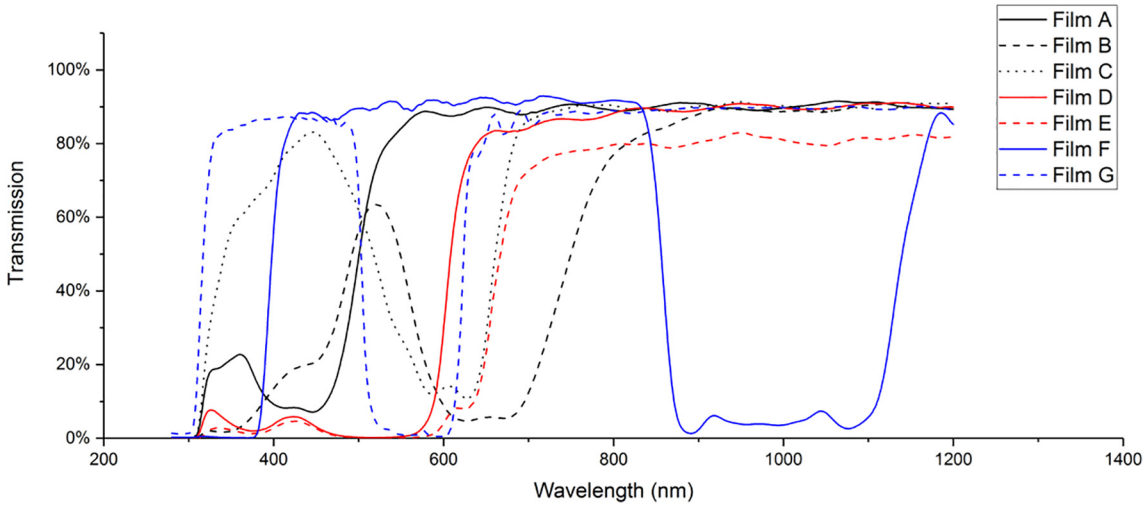

Fig. 3. The transmission spectrum of the films used in the experiment.

Table 2
The proportional parameter k_1, the irradiation S, the temperature T and the series resistance R_s for films A-G.

Film	k_1	S(W/m^2)	T(K)	$R_s(\Omega)$
A	0.7894	900	286	0.06217
B	0.4845	989	287	0.09505
C	0.6727	893	291	0.07518
D	0.5984	945	296	0.07789
E	0.4633	945	294	0.10695
F	0.7001	807	301	0.09026
G	0.6934	882	295	0.07338

$$\gamma = 1 - \frac{V_{oc}}{K_{ph}K_{sh}V_{oc}^{MRC}}(1 - \gamma^{MRC}) \tag{33}$$

$$m = 1 - \frac{1}{\gamma} - \frac{V_{oc}}{N_s n V_T\left(1 - K_s K_{ph}\frac{T}{T^{MRC}}\right) + \frac{K_s K_{ph} V_{oc}^{MRC}\gamma^{MRC}}{\gamma^{MRC}m^{MRC}+1-\gamma^{MRC}}} \tag{34}$$

The short-circuit current I_{sc}^{MRC} and the open-circuit voltage V_{oc}^{MRC} at MRC can be measured directly. Considering that the physical parameters can be changed during the working life [32], the shape parameters m^{MRC} and γ^{MRC} at MRC are extracted by two simple measurements of i for $v = 0.4$ and v for $i = 0.4$ which are chosen differently with Karmalkar S (2008) because of $(v^2 + 1)/2 > v$.

$$\gamma^{MRC} = (i_{v=0.4} - 0.6)/0.4 \tag{35}$$

$$m^{MRC} = \ln\left[\frac{0.6}{\gamma^{MRC}} + \left(1 - \frac{1}{\gamma^{MRC}}\right)v_{i=0.4}\right] / \ln\left(\frac{v_{i=0.4}^2 + 1}{2}\right) \tag{36}$$

Therefore, by using Eqs. (35) and (36), there is only one parameter n to identify the I-V curve under varying conditions. The parameter n is independent of the temperature and irradiation, so it can be received from the datasheet provided by manufacturers as well as the I-V curve at MRC [31].

$$n = \frac{V_{oc}^{MRC}}{V_T^{MRC}}\left(\frac{v_{mp}^{MRC} - \frac{i_{mp}^{MRC}}{1-\gamma^{MRC}+m^{MRC}\gamma^{MRC}} - 1}{m^{MRC}\ln v_{mp}^{MRC} + i_{mp}^{MRC}/\gamma^{MRC}}\right) \tag{37}$$

The maximum point (v_{mp}^{MRC}, i_{mp}^{MRC}) at MRC can be extracted by the formula (19), (20) and the measurements at MRC. Therefore, the identification of I-V characteristic at varying conditions is turned into how to obtain the relationship of the physical parameters between MRC

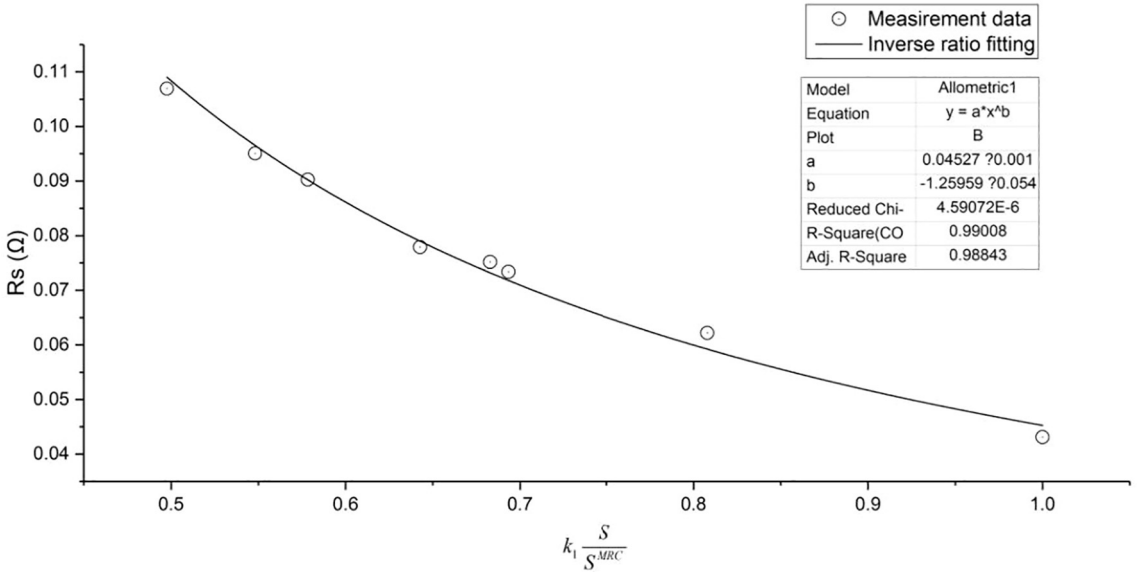

Fig. 4. The relationship between R_s and $k_1\frac{S}{S^{MRC}}$ with inverse fitting ratio.

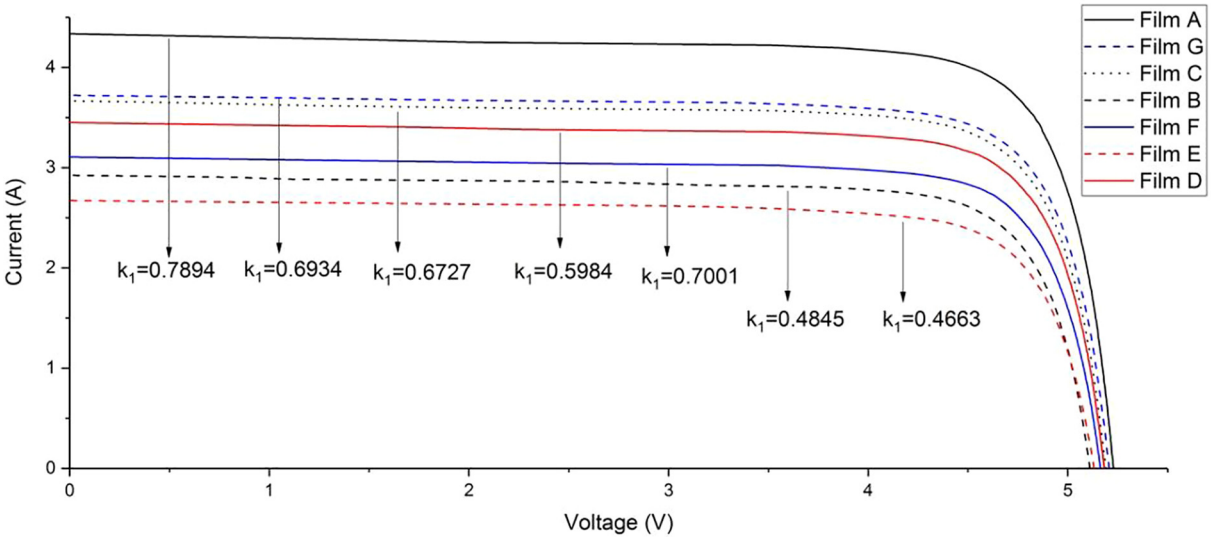

Fig. 5. The I-V curves of film A-G with measurement data.

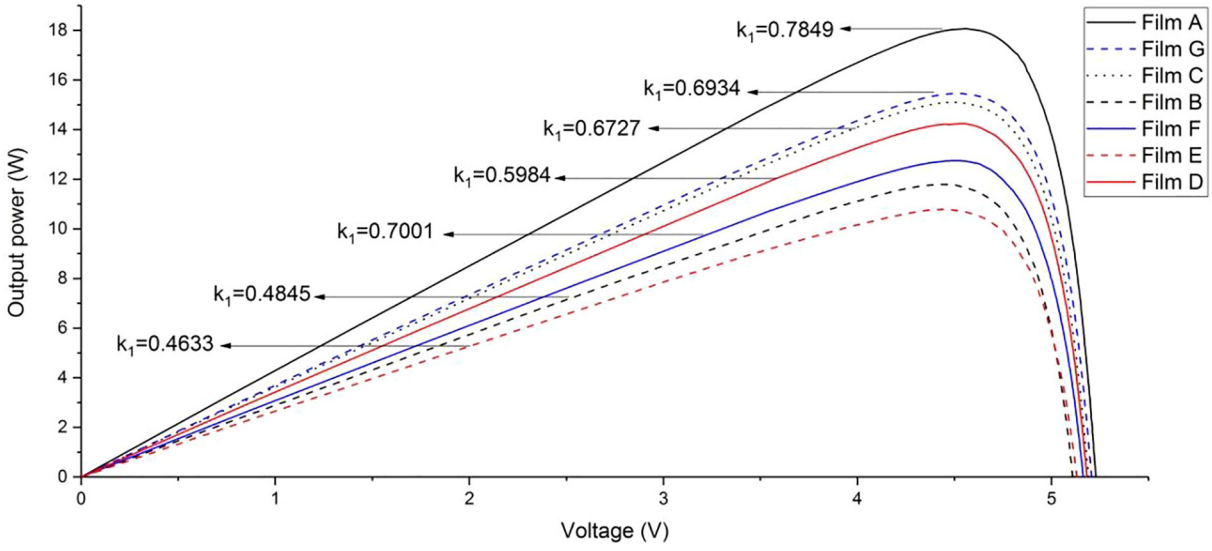

Fig. 6. The P-V curves of film A-G with measurement data.

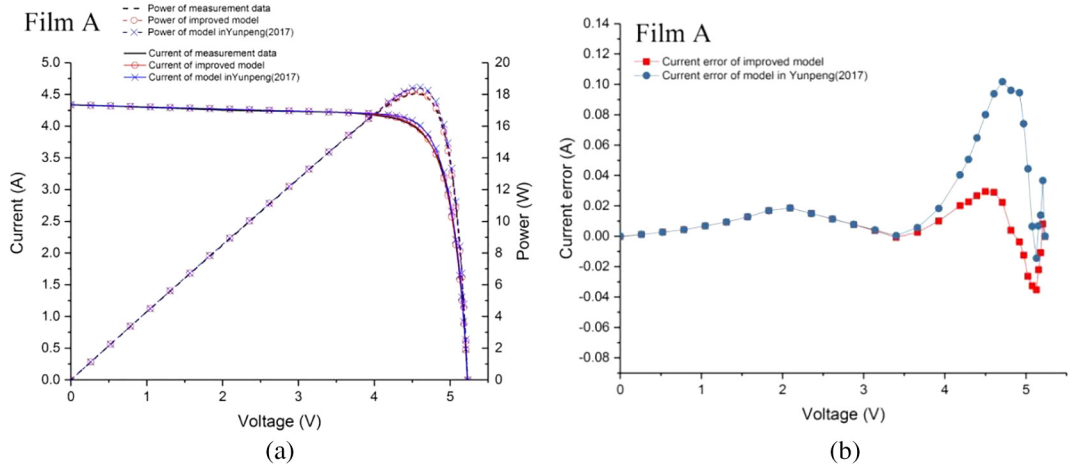

Fig. 7–13. . (a) The curves of film A-G with measurement data, fitted by improved model and model in Yunpeng (2017); (b) The current error curves of two models are also shown in the figure.

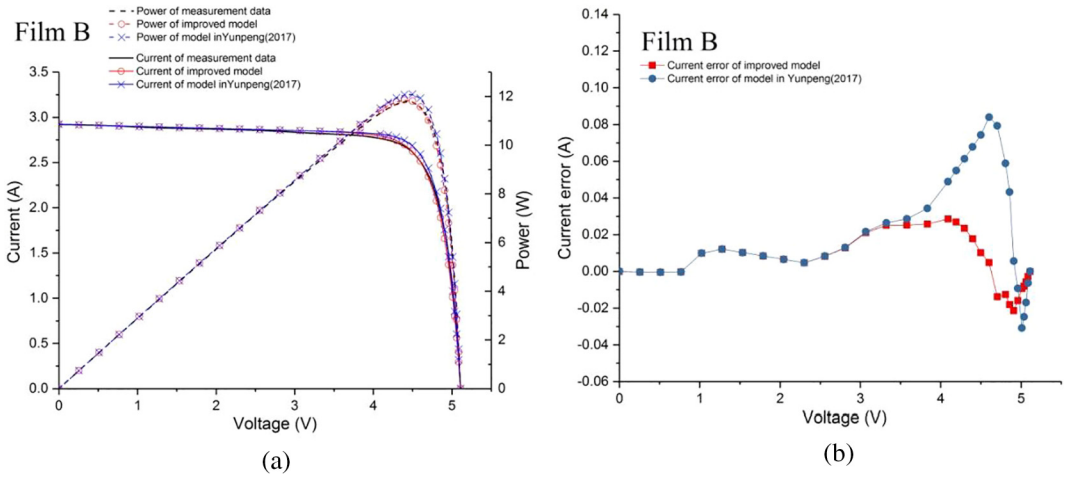

Fig. 7–13. (*continued*)

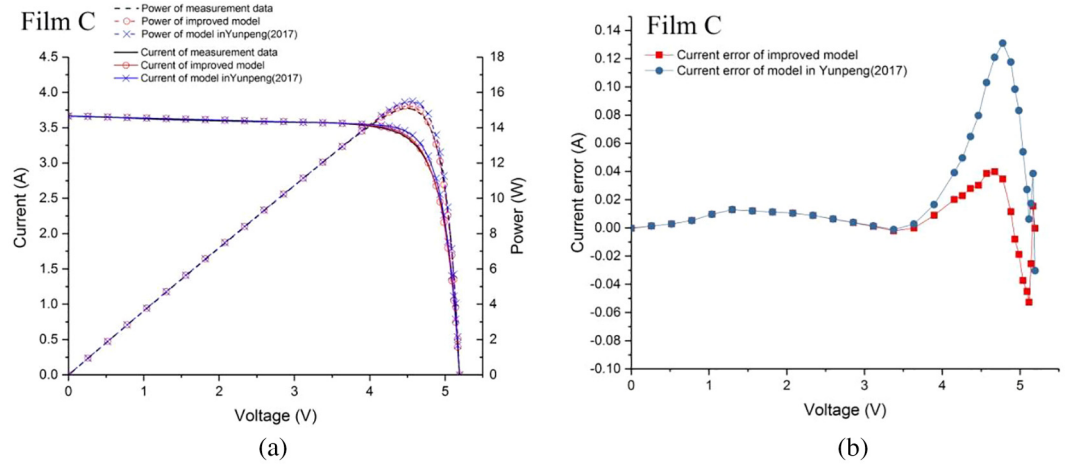

Fig. 7–13. (*continued*)

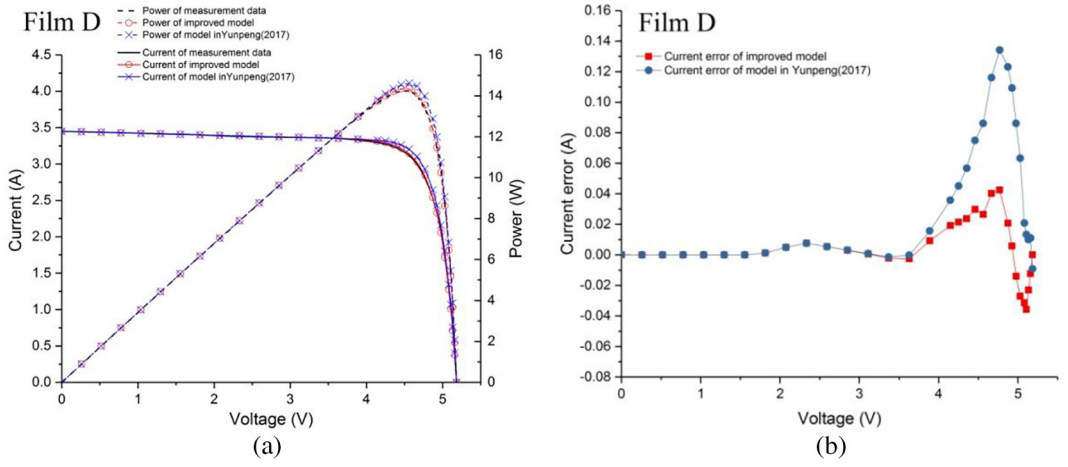

Fig. 7–13. (*continued*)

and varying conditions.

When the spectra of the irradiation are different because of the spectral separation $Spl(\lambda)$ in power generating systems, the changing must be considered with the spectrum response of the solar panels $Rs(\lambda)$ and the solar irradiation spectrum $S(\lambda)$. The spectral ratio parameter k_1 is defined as follow:

$$k_1 = \frac{\int Spe(\lambda)Spl(\lambda)Rs(\lambda)d\lambda}{\int Spe(\lambda)Rs(\lambda)d\lambda} \tag{38}$$

the ratio of the photocurrent K_{ph} and the ratio of the saturation current K_o can be extracted with the temperature [33].

$$K_{ph} = k_1 \cdot \frac{S}{S^{MRC}} \cdot \frac{1 + \alpha_{ph}(T - T^{SRC})}{1 + \alpha_{ph}(T^{MRC} - T^{SRC})} \tag{39}$$

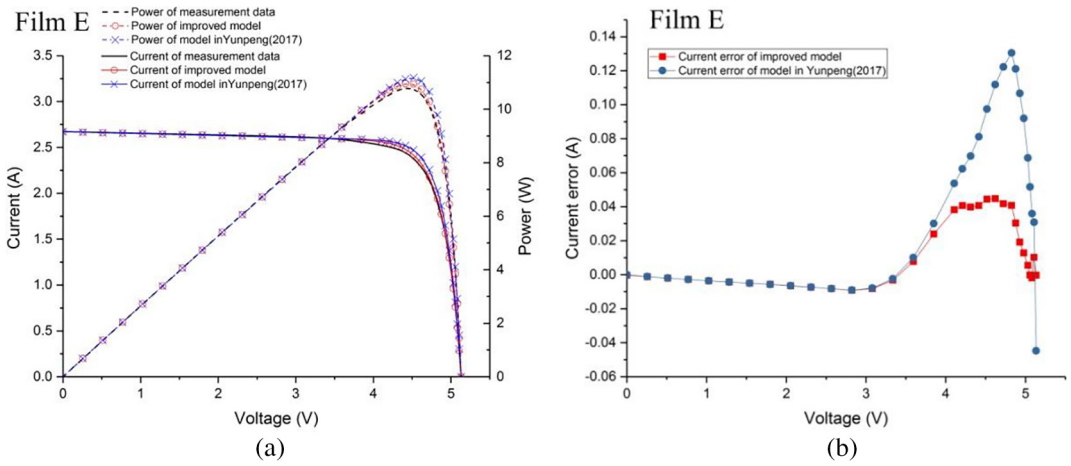

Fig. 7–13. (*continued*)

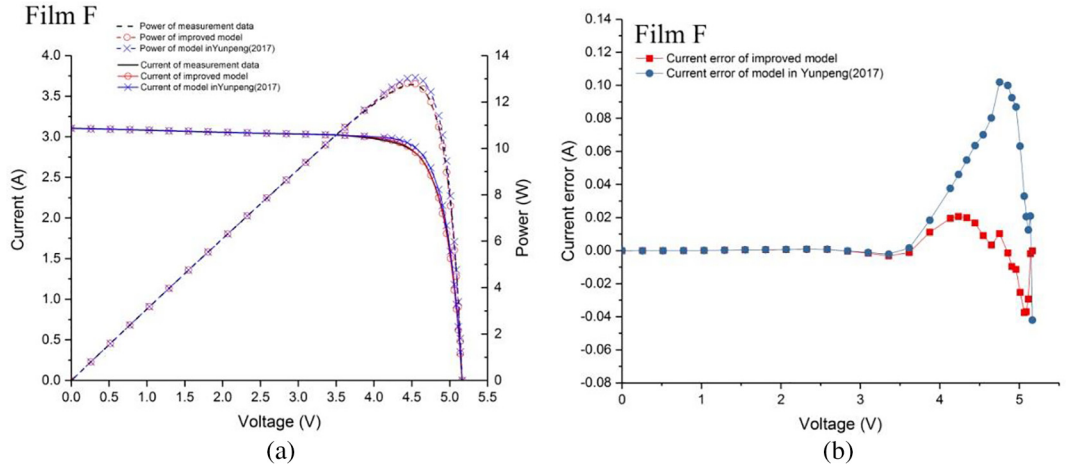

Fig. 7–13. (*continued*)

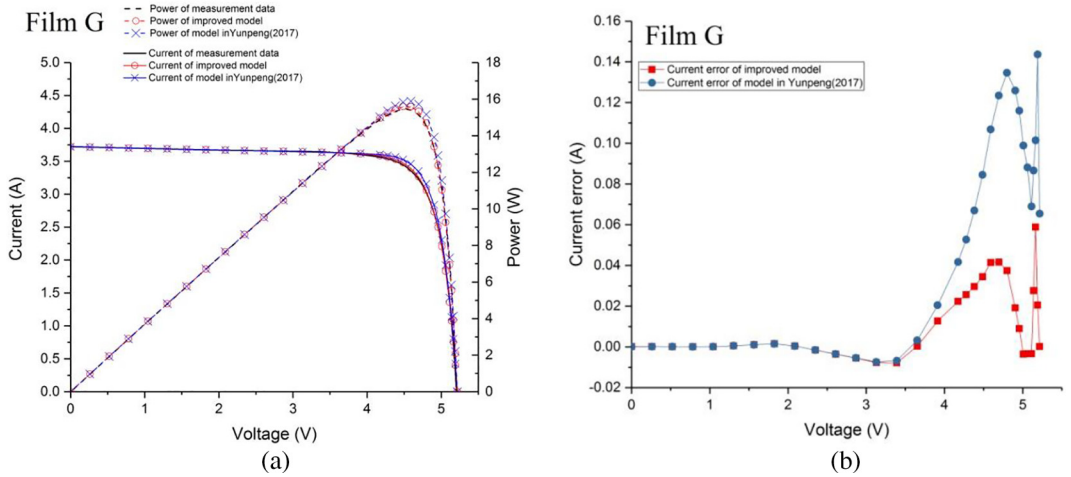

Fig. 7–13. (*continued*)

$$K_0 = \left(\frac{T}{T^{MRC}}\right)^3 \exp\left(\frac{E_g^{MRC}}{kT^{MRC}} - \frac{E_g}{kT}\right) \tag{40}$$

In Eq. (39), the slope of the short-current and temperature α_{ph} can be extracted by the slope of voltage and temperature β_{oc} which both are provided by some manufacturers.

$$\alpha_{ph} \approx \frac{1}{N_s n V_T^{MRC}}\left(\frac{V_T^{MRC}}{T^{MRC}} + \beta_{oc}\right) \tag{41}$$

In Eq. (39), E_g is the band gap of the solar cell materials and exhibits a small temperature dependence. For silicon, E_g can be represented as shown in Soto W D et al. (2006) [32]

$$E_g(T) = E_g(0) - \frac{\alpha_E T^2}{T + \beta} \tag{42}$$

Table 3
The standard deviation of predicted current and power based on improved model and model in Yunpeng (2017).

	Current standard deviation ξ_I (A)		Output power standard deviation ξ_P (W)	
	Improved model	Model in Yunpeng (2017)	Improved model	Model in Yunpeng (2017)
Film A	0.0172	0.0451	0.0771	0.2109
Film B	0.0152	0.0376	0.0608	0.1674
Film C	0.0223	0.0553	0.1053	0.2615
Film D	0.0188	0.0541	0.0893	0.2572
Film E	0.0230	0.0616	0.1031	0.2903
Film F	0.0143	0.0463	0.0693	0.2204
Film G	0.0209	0.0708	0.0997	0.3472

where the $E_g(0) = 1.166$ eV, $\alpha_E = 0.473$ meV/K and $\beta = 636$ K (Zeghbroeck, 2011).

For the shunt resistance of the solar cells, the ratio K_{sh} is used to be considered as S^{MRC}/S [22,24]. But some papers show that most of the shunts are process-induced, such as edge shunts, cracks, holes, scratches or aluminum particles, rather than material induced shunts [34–36]. These effects depend on the carrier in the solar cells related to the irradiation spectrum and the spectral response. In Ruschel C S (2016) [37], the relationship between shunt resistance and irradiation intensity of solar cells made from various materials are presented in different ways. At monocrystalline fitting conditions, the ratio expression for shunt resistance K_{sh} with different irradiation spectra can be expressed as follows:

$$K_{sh} = \left(k_1 \frac{S}{S^{MRC}}\right)^{-0.9} \tag{43}$$

In many papers, the series resistance R_s is considered as a constant which is independent of the temperature and irradiation. However, some researches show that series resistance decreases with irradiation intensity [38,39]. The expression of the relationship between R_s and S hasn't been provided in these papers, so it should be discussed and simulated before any prediction is done.

Results

Validation experiments

The validation experiments were performed with a monocrystalline silicon photovoltaic module. It was composed of 8 photovoltaic cells connected in series. The size of the photovoltaic cells was 12.5 cm × 12.5 cm and were provided by company Sun power. The I-V curve data were measured by Prova-210 measurement-equipment which can scan the I-V curve automatically in one minute. The uncertainty of current is 0.01 A and the uncertainty of voltage is 0.01 V. The solar irradiation and the temperature was monitored with a TES-1333 pyranometer and an infrared thermometer. The measurement error of the TES-1333 pyranometer is 10 W/m^2. The measurement error of infrared thermometer is 1 K.

The experiments were done with sun irradiation at 10 a.m. in November 23, 2017. The I-V curve for the photovoltaic module without film was measured with S = 880 W/m^2 and T = 285 K. The parameters at MRC $V_{oc}{}^{MRC}$, $I_{sc}{}^{MRC}$, $V_{i=0.4}$ and $I_{v=0.4}$ can be derived from the I-V curve directly. The m^{MRC} and γ^{MRC} can be extracted from Eqs. (35) and (36) with the corresponding shape parameters. The shape parameters of the measurement data at MRC are listed in Table 1. It can be verified in Fig. 2 that the improved model with second order approximation is more accurate than the model with first order approximation as discussed in Karmalkar (2008).

There were seven kinds of films used in the experiments. The transmission spectra of the films are shown in Fig. 3. The spectral ratio parameter k_1, the temperature T and the solar irradiation intensity S of the reference condition for each film are listed in Table 2.

The decrease of series resistance R_s is attributed to the increase in conductivity of the active layer. It is caused by the increase of the carriers with the increase in the intensity of illumination. So, the series resistance R_s depend on the term $k_1 \frac{S}{S^{MRC}}$. The relationship is calculated using Matlab software as shown in Fig. 4. The Eq. (44), in which a = 0.04527 Ω and b = −1.26, is proven to be well consistent with the R_s whose regression coefficient is 0.99. The value of the index parameter b is quite different with the value presented in Reich et al. (2009).

$$R_s = a\left(k_1 \frac{S}{S^{MRC}}\right)^b \tag{44}$$

The I-V curves and P-V curves of measurement data are shown in Fig. 5. and Fig. 6. As demonstrated, the output of the solar cells increase with the increasing of spectral ratio parameter k_1. The only abnormal one is the measurement data of film F. It is because that the solar irradiation identity of film F measurement data is much lower than the others.

The prediction of I-V curve under different splitting spectrum

The prediction of I-V curve and P-V curve for the film as it was calculated and discussed by our improved model shown above is compared with the prediction as calculated model in Yunpeng (2017) which used the explicit expression proposed in Karmalkar (2008, 2009).

In Fig. 7–13, the I-V curves and P-V curves of the films A-G with corresponding measurement data are compared with the improved model and the model in Yunpeng (2017). The current error curves are also shown in figures. Furthermore The standard deviation of prediction can be calculated as (45) and (46)

$$\xi_I = \sqrt{\frac{\sum (I_{i,pre} - I_{i,mea})^2}{N-1}} \tag{45}$$

$$\xi_P = \sqrt{\frac{\sum (P_{i,pre} - P_{i,mea})^2}{N-1}} \tag{46}$$

Table 4
Parameter m and maximum power of films A-G with measurement data, improved model and model in Yunpeng (2017).

	Parameter m			Maximum power P_m (W)		
	Measurement data	Improved model	Model in Yunpeng (2017)	Measurement data	Improved model	Model in Yunpeng (2017)
Film A	24.14	23.84	24.77	18.06	18.17	18.46
Film B	22.18	22.77	25.48	11.79	11.96	12.21
Film C	23.45	23.69	25.11	15.10	15.23	15.51
Film D	23.98	24.67	26.22	14.24	14.35	14.62
Film E	22.31	23.86	25.61	10.78	11.11	11.33
Film F	22.94	23.72	25.39	12.75	12.82	13.13
Film G	23.55	23.70	25.08	15.47	15.60	15.89

It is shown in Table 3, the stan1dard deviations of predicted current and power based on improved model are obviously lower than model in Yunpeng (2017). It can be concluded that the improved model has less error than the model in Yunpeng (2017) especially around the maximum power point.

In Table 4, the calculated parameter P_m deriving from the improved model and the model in Yunpeng (2017) are compared with the measurement data. The error is primarily caused by the approximation 3 (see above) with the definition of shape parameters m and the approximation of Eq. (13) after the Taylor expansion. From the figures and tables it gets clear, that the improved model is reliable enough to predict the I-V curve and P-V curve under different irradiation spectra. Thus, the effect of the irradiation spectrum and intensity on the parameters depends on the number of carriers. The error of the temperature and irradiation intensity measurement data causes the error of the I-V and P-V curve as well as the error of $V_{i=0.6}$ and $I_{v=0.6}$ extracted from the I-V curve at MRC. The error caused by the exponential term with v approaches 1 or 0 is not as high as around the maximum power point. In the improved model, the exponential term in the explicit expression is two orders of magnitude approximated instead of just the first order approximation as used in the explicit model of Karmalkar (2008, 2009). Furthermore in Yunpeng (2017), the error is also caused by the value of R_s which considered as a constant independency on the irradiation intensity. In the improved explicit model, the value of R_s is well fitted so that the value of parameter m is more accurate as shown in Table 4.

Conclusion

In this paper we present an explicit I-V model for a PV panel based on the single diode model under different irradiation spectra. The power law of I-V curves which are presented in Karmalkar (2008, 2009) are discussed and calculated combining the single diode model with three approximations. The explicit analyze model is improved as a simple elementary term with second order approximation. To apply the model to the photovoltaic system with spectral separating, the spectrum of the irradiation is taken into account in the model as well. A spectral ratio parameter k_1 extracted from the irradiation spectrum, the transmission spectrum of the film and the spectral response of photovoltaic cells itself are set as a conditional parameter as well as temperature and irradiation intensity. The relationship between the physical parameters and the conditional parameters are discussed and applied to extract the shape parameters at different scenarios. The relationship between R_s and the irradiation intensity as well as the spectrum are discussed and simulated. Furthermore, the condition parameters are used in the explicit analyze model directly to avoid the complex calculation and numerical approximation for the physical parameters as it was done in the single diode model. To avoid the aging effect, the measured I-V parameters from MRC are leveraged instead of the data from SRC, which are provided by the manufacturer. the process of calculation to predict the I-V curve under different splitting spectra is simplified as follow: (1) two shape parameters are gotten from the I-V data at measurement reference conditions (MRC); (2) the short circuit current, open circuit voltage and shape parameters under any splitting spectrum can be calculated based on the relationship provided in article; (3) the performance of PV panel can be predicted with parameters. In the validation experiments, the photovoltaic panel is tested with seven kinds of films. The experimental results showed that there is a good agreement between the calculated and measured I-V curve. The simple elementary term with second order approximation is proved better than the term in Karmalkar S (2008) and Karmalkar S (2009). Furthermore, the improved model has a better prediction of the maximum power compared to the model in Yunpeng (2017). Because of the advantages mentioned above, this model can be widely used for the prediction of I-V characteristic of a PV panel. This model is especially useful for a spectrum splitting system, such as system with various kinds of photovoltaic cells, some kinds of Hybrid Photovoltaic (PV)-Thermoelectric (TE) systems, solar cells used in agriculture and architecture [4,5,11,40]. For the simplicity and validated predictability, this model can be used to design a monitoring software forecast the I-V characteristic for a photovoltaic panel used in a PV system for a long time.

Acknowledgements

This work was supported by The horizontal project between the government of Fuyang city and Teacher college of Fuyang, China. The grand ID is XDHX201724. The measurement of film spectra was done by the Experimental center of USTC (University of Science and Technology of China).

References

[1] Green MA. Recent developments in photovoltaics. Sol Energy 2004;76(1–3):3–8.
[2] Sah CT, Noyce RN, Shockley W. Carrier generation and recombination in P-N junctions and P-N junction characteristics. Proc IRE 1957;45(9):1228–43.
[3] Moon RL, James LW, Vander Plas HA. Multigap solar cell requirements and the performance of AlGaAs and Si cells in concentrated sunlight. 13th Photovoltaic Specialists Conf. 1978:859–67.
[4] Theristis M, Fernández EF, Almonacid F, et al. Spectral Correction of CPV Modules Equipped with GaInP/GaInAs/Ge Solar Cells and Fresnel Lenses. Appl Sci 2017;7(8):842.
[5] Peters M, Goldschmidt JC, Löper P, et al. Spectrally-selective photonic structures for PV applications. Energies 2010;3(2):171–93.
[6] Barnett A, Kirkpatrick D, Honsberg C, et al. Very high efficiency solar cell modules. Prog Photovoltaics Res Appl 2009;17(1):75–83.
[7] Zhao Y, Sheng MY. Design of spectrum splitting solar cell assemblies. Adv Optoelectron Micro/nano-Optics. IEEE. 2011;1–3:2011.
[8] Antonini A, Butturi MA, Zurru P, et al. Development of a high/low concentration photovoltaic module with dichroic spectrum splitting. Prog Photovoltaics Res Appl 2015;23(9):1190–201.
[9] Uzu H, Ichikawa M, Hino M, et al. High efficiency solar cells combining a perovskite and a silicon heterojunction solar cells via an optical splitting system. Appl Phys Lett 2015;106(1):1433–5.
[10] Li G, Shittu S, Diallo TMO, et al. A review of solar photovoltaic-thermoelectric hybrid system for electricity generation. Energy 2018.
[11] Sonneveld PJ, Glam S, Campen J, et al. Performance results of a solar greenhouse combining electrical and thermal energy production. Biosyst Eng 2010;106(1):48–57.
[12] Sonneveld PJ, Swinkels GLAM, Tuijl BAJV, et al. Performance of a concentrated photovoltaic energy system with static linear Fresnel lenses. Sol Energy 2011;85(3):432–42.
[13] Szabo R, Gontean A. Photovoltaic cell and module I-V characteristic approximation using bézier curves. Appl Sci 2018;8(5):2076–3417.
[14] Chin VJ, Salam Z, Ishaque K. Cell modelling and model parameters estimation techniques for photovoltaic simulator application: a review. Appl Energy 2015;154:500–19.
[15] Cubas J, Pindado S, De Manuel C. Explicit expressions for solar panel equivalent circuit parameters based on analytical formulation and the Lambert W-function. Energies 2014;7(7):4098–115.
[16] Necaibia A. A simple theoretical method for the estimation of dynamic resistance in photovoltaic panels. Int J Computer 2012;45(14):21–5.
[17] Chiacchio F, Famoso F, D'Urso D, et al. Dynamic performance evaluation of photovoltaic power plant by stochastic hybrid fault tree automaton model. Energies 2018;11(2):306.
[18] Karmalkar S, Haneefa S. A physically based explicit J-V model of a solar cell for simple design calculations. IEEE Electron Device Lett 2008;29(5):449–51.
[19] Saleem H, Karmalkar S. An analytical method to extract the physical parameters of a solar cell from four points on the illuminated J-V curve. IEEE Electron Device Lett 2009;30(4):349–52.
[20] Das KA. An explicit J-V model of a solar cell for simple fill factor calculation. Sol Energy 2011;85(9):1906–9.
[21] Das KA. An explicit J-V model of a solar cell using equivalent rational function form for simple estimation of maximum power point voltage. Sol Energy 2014;98:400–3.
[22] Lun SX, Du CJ, Guo TT, et al. A new explicit I-V, model of a solar cell based on Taylor's series expansion. Sol Energy 2013;94:221–32.
[23] Lun SX, Du CJ, Sang JS, et al. An improved explicit I-V, model of a solar cell based on symbolic function and manufacturer's datasheet. Sol Energy 2014;110:603–14.
[24] Laudani A, Fulginei FR, Salvini A. Identification of the one-diode model for photovoltaic modules from datasheet values. Sol Energy 2014;108:432–46.
[25] Laudani A, Fulginei FR, Salvini A. High performing extraction procedure for the one-diode model of a photovoltaic panel from experimental I-V curves by using reduced forms. Sol Energy 2014;103(103):316–26.
[26] Jain A, Kapoor A. Exact analytical solutions of the parameters of real solar cells using Lambert W -function. Sol Energy Mater Sol Cells 2004;81(2):269–77.
[27] Ju X, Xu C, Han X, et al. A review of the concentrated photovoltaic/thermal (CPVT) hybrid solar systems based on the spectral beam splitting technology. Appl Energy 2017;187:534–63.
[28] Beeri O, Rotem O, Hazan E, et al. Hybrid photovoltaic-thermoelectric system for

concentrated solar energy conversion: experimental realization and modeling. J Appl Phys 2015;118(11):115104.
[29] Zhang Y, Gao S, Gu T. Prediction of I-V characteristics for a PV panel by combining single diode model and explicit analytical model. Sol Energy 2017;144:349–55.
[30] Karmalkar S, Saleem H. An analytical method to extract the physical parameters of a solar cell from four points on the illuminated J-V curve. IEEE Electron Device Lett 2009;30(4):349–52.
[31] Karmalkar S, Saleem H. The power law J-V, model of an illuminated solar cell. Sol Energy Mater Sol Cells 2011;95(4):1076–84.
[32] Pindado S, Cubas J, Roibás-Millán E, et al. Assessment of explicit models for different photovoltaic technologies. Energies 2018;11(6):1353.
[33] Soto WD, Klein SA, Beckman WA. Improvement and validation of a model for photovoltaic array performance. Sol Energy 2006;80(1):78–88.
[34] Van Zeghbroeck B. Principles of semiconductor devices. Circuits Devices Mag IEEE 2011;22(5):58–9.
[35] Radosavljevic Radovan Lj, Vasic Aleksandra. Effects of radiation on solar cells as photovoltaic generators. Nucl Technol Radiat Prot 2012, 2012,;27(1):28–32.
[36] Breitenstein O, Rakotoniaina JP, Al RMH, et al. Shunt types in crystalline silicon solar cells. Prog Photovoltaics Res Appl 2010;12(7):529–38.
[37] Ruschel CS, Gasparin FP, Costa ER, et al. Assessment of PV modules shunt resistance dependence on solar irradiance. Sol Energy 2016;133:35–43.
[38] Reich NH, van Sark WGJHM, Alsema EA, et al. Crystalline silicon cell performance at low light intensities. Sol Energy Mater Sol Cells 2009;93(9):1471–81.
[39] Khan F, Singh SN, Husain M. Effect of illumination intensity on cell parameters of a silicon solar cell. Sol Energy Mater Sol Cells 2010;94(9):1473–6.
[40] Vasiliev M, Alameh K. Spectrally-selective energy-harvesting solar windows for public infrastructure applications. Applied Sciences 2018;8(6):849.